Supramolecular Chemistry

International Edition: DOI: 10.1002/anie.201709483
German Edition: DOI: 10.1002/ange.201709483

Controlling the Host–Guest Interaction Mode through a Redox Stimulus

György Szalóki, Vincent Croué, Vincent Carré, Frédéric Aubriet, Olivier Alévêque, Eric Levillain, Magali Allain, Juan Aragó, Enrique Ortí, Sébastien Goeb,* and Marc Sallé**

Abstract: *A proof-of-concept related to the redox-control of the binding/releasing process in a host–guest system is achieved by designing a neutral and robust Pt-based redox-active metallacage involving two extended-tetrathiafulvalene (exTTF) ligands. When neutral, the cage is able to bind a planar polyaromatic guest (coronene). Remarkably, the chemical or electrochemical oxidation of the host–guest complex leads to the reversible expulsion of the guest outside the cavity, which is assigned to a drastic change of the host–guest interaction mode, illustrating the key role of counter-anions along the exchange process. The reversible process is supported by various experimental data (^{1}H NMR spectroscopy, ESI-FTICR, and spectroelectrochemistry) as well as by in-depth theoretical calculations performed at the density functional theory (DFT) level.*

The designing of molecular receptors through the metal-driven self-assembly strategy has been actively developed for the last two decades.[1,2] The corresponding guests vary by their size, shape, or charge depending on the targeted application (e.g., sensing, transportation, delivering, or synthesis in confined space).[3] Most of the metallacages are polycationic by nature, as they are usually prepared by the reaction of a neutral polypyridyl ligand and a cationic metal precursor. Consequently, high binding affinities can be observed for anionic guests in organic solvents.[4] In the case of neutral guests, host–guest interactions are by nature more challenging to address.[5] In this context, designing neutral metallacages constitutes an approach with a great potential.[6,4a] We recently demonstrated that neutral polyaromatic species are better bound in the neutral cavity of the Pd-based cage **Pd_4(LTEG)$_2$** than in the related octacationic one **Pd_4(LTEG)$_2^{8+}$**,[6,7] for which **LTEG** corresponds to a π-extended tetrathiafulvalene (exTTF)-based ligand.

Beyond guest binding, much efforts are devoted for controlling the host–guest affinity through an external stimulus.[8,9] The afore-mentioned Pd-based **Pd_4(LTEG)$_2^{8+}$** assembly displays a redox-responsive affinity for an anionic guest, driven by the cage disassembling/assembling process upon oxidation/reduction.[10,11] This is attributed to the severe conformational rearrangement that occurs upon the two-electrons oxidation of each exTTF-based **LTEG** ligand.[12]

To the best of our knowledge, no example of a neutral coordination-cage capable of releasing a neutral guest through a redox stimulus has been described yet. We report herein the synthesis of a neutral and robust platinum-based cage **Pt_4(LTEG)$_2$** that can be oxidized to a stable 4+ state without disassembling, and that allows for the redox-controlled release/binding of the neutral coronene guest. This process, based on a change of the host–guest interaction mode upon oxidation of the cage, illustrates the key role of counter anions. It can be followed by ^{1}H NMR spectroscopy, ESI-FTICR, as well as spectroelectrochemistry, and is supported by theoretical calculations performed at the DFT level.

The cage **Pt_4(LTEG)$_2$** was built from the previously described **LTEG**[10] and the square planar platinum *cis*-diaryl complex [*cis*-Pt(dctfb)$_2$(cod) (dctfb = 3,5-dichloro-2,4,6-trifluorobenzene)] in boiling toluene (Scheme 1). The corresponding ^{1}H NMR spectrum shows upfield shifts of the α/β pyridyl and anthracenyl signals in comparison with the starting ligand, as expected from the ligand-metal coordination (see Figure S3 in the Supporting Information). Diffusion coefficient (D) values of 3.00×10^{-10} m^{2}s^{-1} ($CDCl_3$/CD_3NO_2, (1/1)) and 3.40×10^{-10} m^{2}s^{-1} ($CDCl_3$) were extracted from the ^{1}H DOSY NMR spectra (Figures S4 and S5). Both spectra

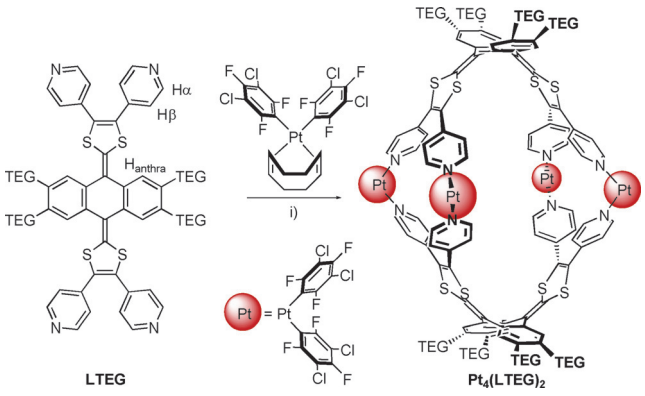

Scheme 1. Synthesis of cage **Pt_4(LTEG)$_2$**. i) Toluene, 110 °C, 8 h, 78 %.

[*] Dr. G. Szalóki, Dr. V. Croué, Dr. O. Alévêque, Dr. E. Levillain, M. Allain, Dr. S. Goeb, Prof. M. Sallé
Université d'Angers, CNRS UMR 6200
Laboratoire MOLTECH-Anjou
2 bd Lavoisier, 49045 Angers Cedex (France)
E-mail: sebastien.goeb@univ-angers.fr
marc.salle@univ-angers.fr
Dr. V. Carré, Prof. F. Aubriet
LCP-A2MC, FR 3624, Université de Lorraine, ICPM
1 boulevard Arago, 57078 Metz Cedex 03 (France)
Dr. J. Aragó, Prof. E. Ortí
Instituto de Ciencia Molecular, Universidad de Valencia
46980 Paterna (Valencia) (Spain)
E-mail: enrique.orti@uv.es
Supporting information and the ORCID identification number(s) for the author(s) of this article can be found under: https://doi.org/10.1002/anie.201709483.

show the presence of only one discrete species in solution with a calculated Stokes radius of 13.4 Å,[13] a value which is in good agreement with the formation of the expected M_4L_2 dimeric structure.[6]

Taking advantage of the cation binding ability of the peripheral TEG chains, we carried out ESI-FTICR studies in presence of KOTf. The observed ionic species $[\mathbf{Pt_4(LTEG)_2}(KOTf)_4\text{-}n OTf]^{n+}$ ($n=4$: $m/z=1302.77$; $n=3$: $m/z=1786.65$; $n=2$: $m/z=2754.48$) and $[\mathbf{Pt_4(LTEG)_2}(KOTf)_3\text{-}2OTf]^{2+}$ ($m/z=2660.52$) confirm the M_4L_2 stoichiometry (Figure S6).

Single crystals of $\mathbf{Pt_4(LTEG)_2}$ were obtained from a $CDCl_3/CD_3CN$ (1/1) solution and the resulting XRD data unambiguously confirmed the ovoid structure of the metallacage (Figure 1 a), with an internal cavity (ca. 15.3 × 12.8 Å) similar to the corresponding palladium analogue (ca. 15.0 × 13.0 Å).[6]

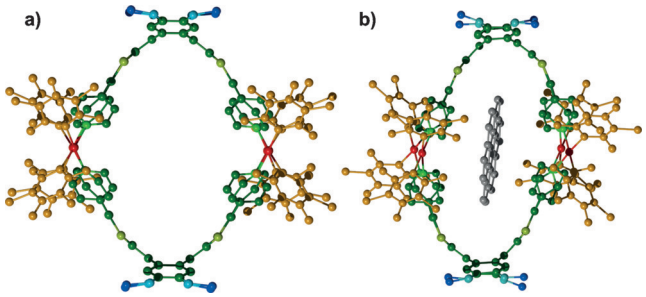

Figure 1. X-ray crystal structure of a) $\mathbf{Pt_4(LTEG)_2}$ (the disorder did not allow for resolution of TEG chains) and b) Coronene⊂$\mathbf{Pt_4(LTEG)_2}$ (TEG chains are omitted for clarity).

As anticipated,[14] the newly synthesized platinum cage presents a highly improved stability over the corresponding neutral palladium analogue $\mathbf{Pd_4(LTEG)_2}$. This is first reflected in the more demanding conditions required for the synthesis of $\mathbf{Pt_4(LTEG)_2}$ versus the corresponding Pd cage (toluene, 110 °C vs. acetone, r.t.),[6] and was corroborated by a comparative ^{1}H NMR stability experiment (Figure S7). Whereas no degradation of the $\mathbf{Pt_4(LTEG)_2}$ assembly was observed upon standing in $CDCl_3$ after 14 days, an evolution product appeared after one day in the case of $\mathbf{Pd_4(LTEG)_2}$ assigned to a M_6L_3 species (Figures S8 and S9).[15]

The electrochemical properties of $\mathbf{Pt_4(LTEG)_2}$, as well as of $\mathbf{Pd_4(LTEG)_2}$ and **LTEG** for comparison (see Figure 2), were studied by cyclic voltammetry in CH_2Cl_2/CH_3CN (1/1). As usually observed for exTTF derivatives, **LTEG** exhibits a pseudo-reversible wave, located at $E_1^{ox}=0.04$ V versus Fc/Fc$^+$. The oxidation wave is shifted to $E_1^{ox}=0.28$ V in the case of $\mathbf{Pd_4(LTEG)_2}$ as expected from coordination to the metal. Interestingly, the corresponding reduction process at $E_1^{red}=-0.09$ V occurs at the same potential as for the free ligand **LTEG**. This behavior suggests, as already observed for the homologous octacationic $\mathbf{Pd_4(LTEG)_2}^{8+}$ cage,[10] that a disassembling of the neutral Pd cage occurs upon oxidation. In addition, the voltammogram of $\mathbf{Pd_4(LTEG)_2}$ appears unchanged upon several cycles, indicating the reversible character of the disassembling/assembling process. A striking different behavior is observed for the voltammogram of the Pt

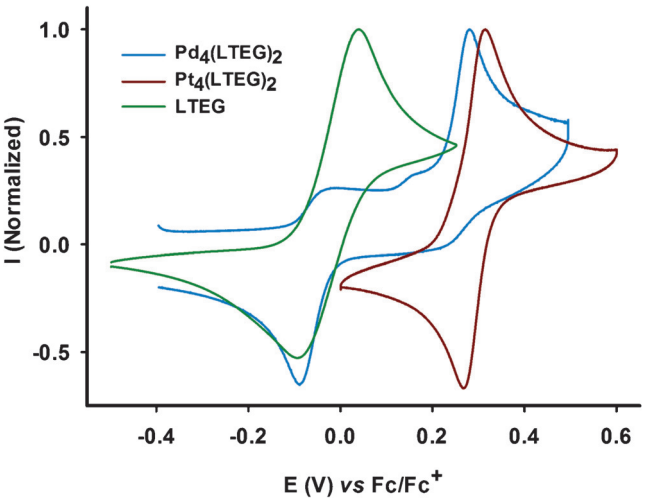

Figure 2. Cyclic voltammogram of ligand **LTEG** and cages $\mathbf{Pt_4(LTEG)_2}$ and $\mathbf{Pd_4(LTEG)_2}$, $c=10^{-4}$ M in 0.1 M $TBAPF_6$ (CH_2Cl_2/CH_3CN (1/1)), 100 mV s^{-1}.

cage, $\mathbf{Pt_4(LTEG)_2}$, which exhibits a quasi-reversible oxidation wave at $E_1^{ox}=0.32$ V versus Fc/Fc$^+$. Such a difference between two neutral M_4L_2 cages which only differ by their metal center (M) is assigned to the more robust character of the Pt-pyridine bond versus the Pd-pyridine bond. The reversible nature of the redox process in the case of $\mathbf{Pt_4(LTEG)_2}$ suggests the absence of exTTF conformational change due to the rigidification of the system[16] and, most importantly, the absence of disassembling of the cage during the oxidation process. This is also confirmed by a thin layer cyclic voltammetry (TLCV) experiment (Figure S10), which shows that both exTTF moieties are reversibly oxidized into their dicationic state.

The higher strength of the Pt–N bond compared to the Pd–N bond was studied by DFT calculations on Pt versus Pd metallacages (see the Supporting Information, Figures S27, S28 and S31). Dissociation energies of 98.6 and 89.6 kcal mol^{-1} are estimated at the B3LYP-D3/(6-31G** + LANL2DZ) level for the $\mathbf{Pt_4(LTEG)_2}$ and $\mathbf{Pd_4(LTEG)_2}$ cages, respectively. DFT calculations also indicate that a stable tetracation Pt-cage $\mathbf{Pt_4(LTEG^{2+})_2}$ is formed upon oxidation (Figure S32). The ovoid cavity slightly changes in passing from the neutral complex (16.2 × 10.6 Å) to the tetracation (15.4 × 12.5 Å), and the charge is mainly extracted from the **LTEG** ligands (1.95e from each ligand). See the Supporting Information for a full discussion of how the structural parameters of the cage change upon oxidation.

The redox behavior of $\mathbf{Pt_4(LTEG)_2}$ was also investigated by chemical oxidation/reduction and followed by ^{1}H NMR (Figure 3). Upon oxidation with $AgBF_4$, a strong downfield shift of the corresponding α/β-pyridyl and anthracenyl signals is observed (Figure 3 b). This important deshielding effect results from the electron deficient character of both dicationic exTTF moieties. In addition, the presence of uncoordinated oxidized ligand $(\mathbf{LTEG})^{2+}$ was ruled out (Figure S11 and data below). Subsequent reduction of the resulting species with TDAE (TDAE = tetrakis(dimethylamino)ethylene) allows to integrally recover the initial neutral cage species (Figure 3 c).

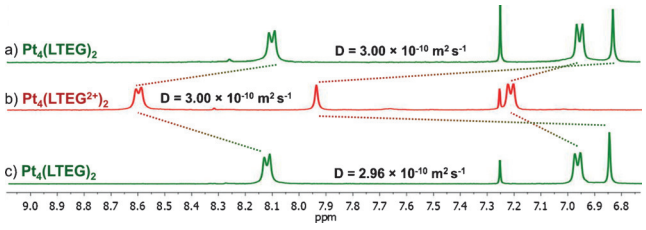

Figure 3. ^{1}H NMR ($CDCl_3/CD_3NO_2$ (1/1), 298 K, 2 mM) downfield region of a) **$Pt_4(LTEG)_2$**, b) after addition of 14 equiv of $AgBF_4$, and c) after subsequent addition of 10 equiv of TDAE.

Finally, ^{1}H DOSY NMR experiments reveal that the size of the neutral and oxidized species are similar ($D = 3.00 \times 10^{-10}\ m^2 s^{-1}$), which supports the assumption of a reversible oxidation process without disassembly of the cage (Figures S4, S12 and S13). The integrity of the **$Pt_4(LTEG^{2+})_2$** oxidized cage was additionally confirmed by ESI-FTICR measurements upon addition of either thianthrenium tetrafluoroborate or silver tetrafluoroborate oxidants to the neutral cage **$Pt_4(LTEG)_2$** (Figures S14 and S15).

Having in hands a redox-active metallacage which does not disassemble upon oxidation, we were interested in the study of the redox-controlled release/uptake of a neutral polyaromatic guest molecule. The title platinum cage forms a strong host–guest complex with coronene, which was characterized in solution with significant upfield shifts of the pyridyl signals compared to the empty cage, due to the aromatic shielding effects of the encapsulated coronene. An association constant of $K_a = 8.6 \times 10^3\ M^{-1}$ in $CDCl_3/CD_3NO_2$ (1/1) was determined from a DOSY NMR titration (Figures S16 and S17). The host–guest complex was also characterized in the solid state by X-Ray crystallography (Figure 1b). The cavity size is somewhat modified related to the free host, with values evolving from 15.3 × 12.8 Å (**$Pt_4(LTEG)_2$**) to 16.2 × 10.6 Å (Coronene⊂**$Pt_4(LTEG)_2$**), illustrating the unexpectedly high flexible nature of the cage. After addition of $AgBF_4$ (oxidant) to the Coronene⊂**$Pt_4(LTEG)_2$** complex (Figure 4a), the ^{1}H NMR spectrum revealed two set of signals corresponding to the sum of the oxidized cage **$Pt_4(LTEG^{2+})_2$** (see Figure 3b) and of free coronene (Figures 4b and S16). The corresponding DOSY NMR study exhibits consistent diffusion values of $2.95 \times 10^{-10}\ m^2 s^{-1}$ and $12.4 \times 10^{-10}\ m^2 s^{-1}$, respectively (Figure S18). The former proves the complete oxidation of the metallacage, whereas the latter justifies the ejection of the guest molecule. Finally,

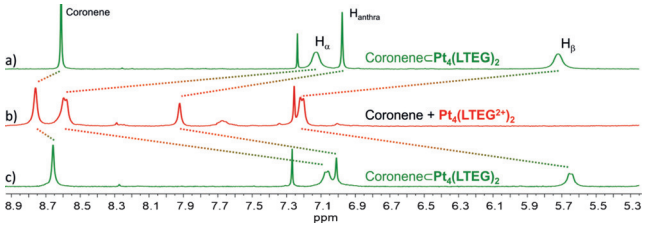

Figure 4. ^{1}H NMR ($CDCl_3/CD_3NO_2$ (1/1), 298 K, 2 mM) downfield region of a) a stoichiometric mixture of **$Pt_4(LTEG)_2$** and coronene (Coronene⊂**$Pt_4(LTEG)_2$** complex), b) after addition of 12 equiv of $AgBF_4$, and c) after subsequent addition of 12 equiv of TDAE.

the original host–guest complex is restored upon reduction with TDAE (Figures 4c and S17–S19).

This reversible uptake/release redox-controlled process is also supported by ESI-FTICR measurements. While a stoichiometric solution of **$Pt_4(LTEG)_2$** and coronene in presence of KOTf provides almost exclusively signals corresponding to the host–guest complex ($m/z = 1378.04$, 1887.02, 2904.53) (Figure S20), only the empty **$Pt_4(LTEG^{2+})_2$** metallacage was observed after addition of an excess of oxidant (Figures S21 and S23). Finally, the characteristic signals of the original host–guest inclusion complex were recovered after reduction with TDAE (Figures S22 and S24).

To get a better understanding of the coronene uptake/release process, the neutral Coronene⊂**$Pt_4(LTEG)_2$** and oxidized Coronene⊂**$Pt_4(LTEG^{2+})_2$** host–guest complexes were optimized at the B3LYP-D3/(6-31G** + LANL2DZ) level. Calculations predict that the inclusion of coronene provokes a reduction in the cage dimensions (Figure S35), as it is also observed in the X-ray structures (Figure 1). Similar coronene-cage stabilizing interaction energies of −101.3 and −95.6 kcal mol^{-1} were computed for Coronene⊂**$Pt_4(LTEG)_2$** and Coronene⊂**$Pt_4(LTEG^{2+})_2$** complexes, respectively, which do not justify the observed experimental difference in host–guest properties of the neutral versus the charged (oxidized) cage. Importantly, it should be taken into account that counter-anions are also present upon cage oxidation with $AgBF_4$. Complexes formed by the charged **$Pt_4(LTEG^{2+})_2$** cage interacting with four BF_4^- anions in different orientations were therefore optimized (Figure 5 and S36). The complex

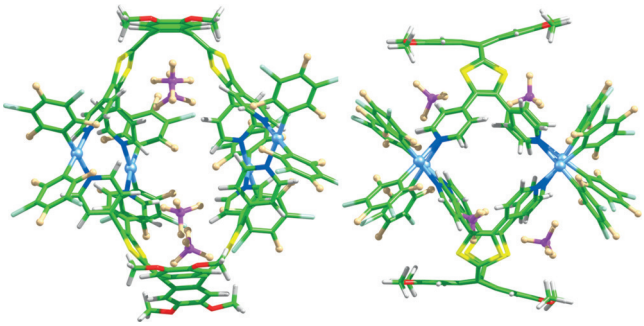

Figure 5. Side views of the optimized structure computed at the B3LYP-D3/(6-31G** + LANL2DZ) level in CH_3CN for the charged **$Pt_4(LTEG^{2+})_2$** cage interacting with four BF_4^- anions inside the cavity.

with four BF_4^- anions inside the cavity shown in Figure 5 was found to be the most stable structure and presents an interaction energy of −122.8 kcal mol^{-1}, which is significantly higher than that obtained for the Coronene⊂**$Pt_4(LTEG^{2+})_2$** complex (−95.6 kcal mol^{-1}). Such observation was expected from the attractive electrostatic interactions occurring between the positively charged cavity and the anions, resulting in the displacement of coronene outside the cavity. B3LYP-D3 calculations therefore indicates that the insertion of the counter-anions in the cavity is responsible for the release of the coronene guest.

Finally, the capability of the **$Pt_4(LTEG)_2$** cage to modulate the binding properties depending on its charge state was

followed in real-time using a spectroelectrochemical setup (Figure 6).[17] As a complementary approach to the above studies which focused on the host unit, the expulsion/complexation process was monitored by probing the coronene guest. The experiment is based on the variation of the fluorescence properties of coronene, which are developed when the guest is free, but quenched when encapsulated. The fluorescence response resulting from an equimolar solution of **$Pt_4(LTEG)_2$** and coronene ($\lambda_{exc} = 300$ nm centered on the guest) was recorded during a cyclic voltammetry measurement. The fluorescence intensity of the host–guest system is of 28 intensity units at 450 nm, and increases to 46 intensity units (+65%) during the oxidation step of **$Pt_4(LTEG)_2$** (Figure 6). Noteworthy, the initial intensity of the signal is recovered after reduction. This result is in good agreement with the NMR and MS analysis as well as with computational studies and supports the reversible redox-controlled release/uptake of the coronene guest. It should be noted that no modulation of the coronene fluorescence occurs under the same conditions in absence of the **$Pt_4(LTEG)_2$** host (Figure S25).

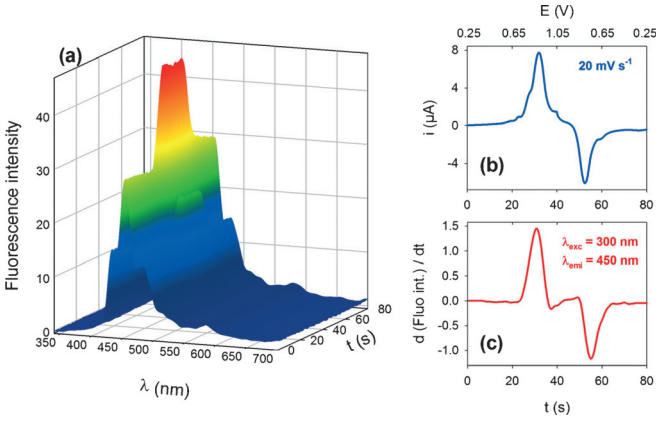

Figure 6. Fluorescence evolution of an equimolar solution of **$Pt_4(LTEG)_2$** and coronene (coronene⊂**$Pt_4(LTEG)_2$** complex) followed by a thin layer spectroelectrochemical experiment a) $c = 10^{-4}$ M in 0.1 M NBu_4PF_6 (CH_2Cl_2/CH_3CN (1/1)), 20 mV s^{-1} on Pt electrode. Comparison between TLCV at 20 mV s^{-1} (b) and [d(fluorescence intensity)/dt] at 450 nm (c), extracted from the spectroelectrochemical experiment.

A similar experiment carried out using NBu_4BArF (tetra-*n*-butylammonium tetrakis[3,5-bis(trifluoromethyl)phenyl]-borate) as supporting electrolyte, results in an increase of the fluorescence intensity of only 24% (Figure S26). Such a significant difference with the previous experiment is assigned to the size of the counter-anion. While PF_6^- can easily penetrate the oxidized cavity and drives out the encapsulated neutral coronene guest, the much bigger $BArF^-$ anion (diameter of ca. 11.5 Å) cannot enter the cavity. This behavior is consistent with our previous findings related to the strong influence of the anion size over the guest complexation in a polycationic cage[6] and corroborates the role of the anion in the encapsulation process.[18]

In summary, a novel neutral electroactive M_4L_2 (M = Pt) metallacage was designed to support without disassembling the reversible generation of positive charges over the cavity upon oxidation. The resulting neutral Pt cage appears significantly more robust than the Pd analogue and shows a good ability to bind one coronene guest, giving rise to a fully neutral host–guest complex. Importantly, this system allows to demonstrate that controlling the cavity charge from 0 to 4+ leads to a triggering of the binding/release of the neutral guest.[19] This process control is assigned to an original change of the host–guest interaction mode when switching from a neutral cavity to a positively charged one, with a critical role played by the counter anion present in solution. The latter are prone to strongly interact with the positively charged cavity, leading to the displacement of the neutral guest outside the cavity. Enlarging the scope of this original redox-based approach to alternative metallacages is underway.

Acknowledgements

This work was supported by the ANR JCJC program (ANR-14-CE08-0001 BOMBER), the Spanish Ministry of Economy and Competitiveness MINECO (CTQ2015-71154-P and Unidad de Excelencia María de Maeztu MDM-2015-0538), the Generalitat Valenciana (PROMETEO/2016/135), and European FEDER funds (CTQ2015-71154-P). The authors gratefully acknowledge the PIAM (Univ. Angers). J.A. is grateful to MINECO for a "JdC-incorporación" post-doctoral fellowship.

Conflict of interest

The authors declare no conflict of interest.

Keywords: cage compounds · host–guest systems · self-assembly · supramolecular chemistry · tetrathiafulvalene

How to cite: *Angew. Chem. Int. Ed.* **2017**, *56*, 16272–16276
Angew. Chem. **2017**, *129*, 16490–16494

[1] M. Fujita, J. Yazaki, K. Ogura, *J. Am. Chem. Soc.* **1990**, *112*, 5645–5647.
[2] a) S. Zarra, D. M. Wood, D. A. Roberts, J. R. Nitschke, *Chem. Soc. Rev.* **2015**, *44*, 419–432; b) J. J. Henkelis, M. J. Hardie, *Chem. Commun.* **2015**, *51*, 11929–11943; c) T. R. Cook, P. J. Stang, *Chem. Rev.* **2015**, *115*, 7001–7045; d) L. Chen, Q. Chen, M. Wu, F. Jiang, M. Hong, *Acc. Chem. Res.* **2015**, *48*, 201–210; e) M. Yoshizawa, J. K. Klosterman, *Chem. Soc. Rev.* **2014**, *43*, 1885–1898; f) S. Mukherjee, P. S. Mukherjee, *Chem. Commun.* **2014**, *50*, 2239–2248; g) M. Han, D. M. Engelhard, G. H. Clever, *Chem. Soc. Rev.* **2014**, *43*, 1848–1860; h) M. M. J. Smulders, I. A. Riddell, C. Browne, J. R. Nitschke, *Chem. Soc. Rev.* **2013**, *42*, 1728–1754; i) N. B. Debata, D. Tripathy, D. K. Chand, *Coord. Chem. Rev.* **2012**, *256*, 1831–1945.
[3] a) D.-H. Qu, Q.-C. Wang, Q.-W. Zhang, X. Ma, H. Tian, *Chem. Rev.* **2015**, *115*, 7543–7588; b) N. Ahmad, H. A. Younus, A. H. Chughtai, F. Verpoort, *Chem. Soc. Rev.* **2015**, *44*, 9–25; c) B. Therrien, in *Nanomaterials in Drug Delivery, Imaging, and Tissue Engineering*, Wiley, Hoboken, **2013**, pp. 145–166; d) B. Therrien, *Chem. Nanocontainers* **2011**, *319*, 35–55; e) H. Amouri, C. Desmarets, J. Moussa, *Chem. Rev.* **2012**, *112*, 2015–2041.

[4] a) P. Thanasekaran, C.-H. Lee, K.-L. Lu, *Coord. Chem. Rev.* **2014**, *280*, 96 – 175; b) R. Chakrabarty, P. S. Mukherjee, P. J. Stang, *Chem. Rev.* **2011**, *111*, 6810 – 6918.
[5] a) D. B. Varshey, J. R. G. Sander, T. Friščić, L. R. MacGillivray, in *Supramol. Chem.*, Wiley, Hoboken, **2012**; b) M. Yoshizawa, M. Yamashina, *Chem. Lett.* **2017**, *46*, 163 – 171; c) M. Yoshizawa, J. Nakagawa, K. Kumazawa, M. Nagao, M. Kawano, T. Ozeki, M. Fujita, *Angew. Chem. Int. Ed.* **2005**, *44*, 1810 – 1813; *Angew. Chem.* **2005**, *117*, 1844 – 1847.
[6] G. Szalóki, V. Croué, M. Allain, S. Goeb, M. Sallé, *Chem. Commun.* **2016**, *52*, 10012 – 10015.
[7] S. Bivaud, S. Goeb, V. Croue, P. I. Dron, M. Allain, M. Sallé, *J. Am. Chem. Soc.* **2013**, *135*, 10018 – 10021.
[8] a) W. Wang, Y.-X. Wang, H.-B. Yang, *Chem. Soc. Rev.* **2016**, *45*, 2656 – 2693; b) A. J. McConnell, C. S. Wood, P. P. Neelakandan, J. R. Nitschke, *Chem. Rev.* **2015**, *115*, 7729 – 7793.
[9] For illustrative examples see: a) S. T. J. Ryan, J. del Barrio, R. Suardíaz, D. F. Ryan, E. Rosta, O. A. Scherman, *Angew. Chem. Int. Ed.* **2016**, *55*, 16096 – 16100; *Angew. Chem.* **2016**, *128*, 16330 – 16334; b) N. Kishi, M. Akita, M. Yoshizawa, *Angew. Chem. Int. Ed.* **2014**, *53*, 3604 – 3607; *Angew. Chem.* **2014**, *126*, 3678 – 3681; c) M. Han, R. Michel, B. He, Y. S. Chen, D. Stalke, M. John, G. H. Clever, *Angew. Chem. Int. Ed.* **2013**, *52*, 1319 – 1323; *Angew. Chem.* **2013**, *125*, 1358 – 1362; d) J. E. M. Lewis, E. L. Gavey, S. A. Cameron, J. D. Crowley, *Chem. Sci.* **2012**, *3*, 778 – 784; e) I. A. Riddell, M. M. J. Smulders, J. K. Clegg, J. R. Nitschke, *Chem. Commun.* **2011**, *47*, 457 – 459; f) T. Murase, S. Sato, M. Fujita, *Angew. Chem. Int. Ed.* **2007**, *46*, 5133 – 5136; *Angew. Chem.* **2007**, *119*, 5225 – 5228.
[10] V. Croué, S. Goeb, G. Szalóki, M. Allain, M. Sallé, *Angew. Chem. Int. Ed.* **2016**, *55*, 1746 – 1750; *Angew. Chem.* **2016**, *128*, 1778 – 1782.
[11] For a recent study on a redox-induced switching between coordination self-assemblies, see: M. J. Burke, G. S. Nichol, P. J. Lusby, *J. Am. Chem. Soc.* **2016**, *138*, 9308 – 9315.
[12] The conformation evolves from a butterfly shape (neutral state) to a fully aromatic system for which both aromatic dithiolium rings are perpendicular to the anthracene backbone. a) F. G. Brunetti, J. L. Lopez, C. Atienza, N. Martin, *J. Mater. Chem.* **2012**, *22*, 4188 – 4205; b) A. J. Moore, M. R. Bryce, *J. Chem. Soc. Perkin Trans. 1* **1991**, *0*, 157 – 168; c) M. R. Bryce, A. J. Moore, M. Hasan, G. J. Ashwell, A. T. Fraser, W. Clegg, M. B. Hursthouse, A. I. Karaulov, *Angew. Chem. Int. Ed. Engl.* **1990**, *29*, 1450 – 1452; *Angew. Chem.* **1990**, *102*, 1493 – 1495.
[13] a) L. Avram, Y. Cohen, *Chem. Soc. Rev.* **2015**, *44*, 586 – 602; b) A. Macchioni, G. Ciancaleoni, C. Zuccaccia, D. Zuccaccia, *Chem. Soc. Rev.* **2008**, *37*, 479 – 489.
[14] F. Ibukuro, T. Kusukawa, M. Fujita, *J. Am. Chem. Soc.* **1998**, *120*, 8561 – 8562.
[15] S. Bivaud, S. Goeb, V. Croué, M. Allain, F. Pop, M. Sallé, *Beilstein J. Org. Chem.* **2015**, *11*, 966 – 971.
[16] S.-G. Liu, I. Pérez, N. Martín, L. Echegoyen, *J. Org. Chem.* **2000**, *65*, 9092 – 9102.
[17] a) O. Alévêque, E. Levillain, in *Luminescence in Electrochemistry: Applications in Anal. Chem. Physics and Biology* (Eds.: F. Miomandre, P. Audebert), Springer, Cham, **2017**, pp. 1 – 19; b) S. Bkhach, Y. Le Duc, O. Alévêque, C. Gautier, P. Hudhomme, E. Levillain, *ChemElectroChem* **2016**, *3*, 887 – 891; c) M. Dias, P. Hudhomme, E. Levillain, L. Perrin, Y. Sahin, F.-X. Sauvage, C. Wartelle, *Electrochem. Commun.* **2004**, *6*, 325 – 330.
[18] D. P. August, G. S. Nichol, P. J. Lusby, *Angew. Chem. Int. Ed.* **2016**, *55*, 15022 – 15026; *Angew. Chem.* **2016**, *128*, 15246 – 15250.
[19] A coordination cage allowing a redox modulation of the cavity charge state was recently described, but did not exhibit a control over the host – guest binding. K. Yazaki, S. Noda, Y. Tanaka, Y. Sei, M. Akita, M. Yoshizawa, *Angew. Chem. Int. Ed.* **2016**, *55*, 15031 – 15034; *Angew. Chem.* **2016**, *128*, 15255 – 15258.

Manuscript received: September 13, 2017
Accepted manuscript online: October 30, 2017
Version of record online: November 23, 2017

